Cooperation between Humans and Robots Underwater

André Potes*, David Cabecinhas* and António Pascoal*
*ISR/IST, University of Lisbon, Lisbon, Portugal.

***Abstract*—In underwater environments, human divers face enormous challenges commonly related to poor visibility, lack of orientation, heavy equipment, limited breathing time and pressure-related issues. This does not only hinder the diver's work performance but also increases the probabilities of occurring accidents. With this in mind, the present work addresses the problem of enabling cooperative strategies between the diver and autonomous underwater vehicle (AUV) aiming to increase task safety and efficiency levels. From a practical perspective, our work contributes by proposing a cooperation architecture between a diver and the AUV guidance, navigation and control systems. Under this cooperation framework, we present state of the art solutions to localize and track the diver via algorithms and onboard sensors of the AUV and follow up by designing its control system. From a theoretical perspective, the derivation of the controllers exploit nonlinear Lyapunov based techniques and geometric control analysis tools, achieving robust properties and stable equilibria that are proved formally. Simulations results are presented and discussed, in the presence of measurement noise, constant ocean current disturbances and uncertainty in the model parameters of our vehicle, illustrating the performance achieved with the proposed control system in a realistic cooperative scenario with a diver.**

***Index Terms*—Autonomous underwater vehicles, Diver-robot interaction, Geometric control, Path following, Stability of nonlinear systems, Target tracking.**

I. INTRODUCTION

Diving has come a long way since humans started exploring underwater environments. These activities were and still are motivated by the exploitation of marine resources and exploring unknown areas, which still cover a large percentage of our aquatic planet. During the maturing process along these years, diving experience has shown that, in contrast with other land-based activities, is not easily performed, and ultimately requires extreme caution and standardised procedures to minimise risk faced by divers [1]. For this reason, there has recently been an interest in developing new strategies and work ethics in carrying out these diving operations, which raises the question of whether the use of cooperative mechanisms between divers and robots can increase efficiency and reduce risk levels. Moreover, the marine environment raises several challenges and opportunities for new solutions embedded in navigation and control literature [2]. Applications of these mechanisms will surely result in solutions to problems in the field of robotics and lead to new questions, producing cyclical research and development work, boosting innovation and contributing towards science.

Cooperation strategies can be enacted in various different solutions, but the present thesis focuses on the guidance, navigation and control solutions applied to autonomous underwater vehicles (AUVs), partially motivated with state of the art solutions regarding the problem of target tracking [3], [4], localization [5]–[7] and nonlinear control [8]–[12]. Together with the nonexistence of tether cables and human element, always present in remotely operated vehicles (ROVs), this paves the ground to robust and efficient autonomous architectures. Previous works [13]–[17] were carried out under many objectives but with the common goal of developing and researching cooperation frameworks between autonomous marine vehicles (AMRVs) and divers, and serve as a basis of guidance and support to this work. In summary, this paper addresses the problem of *designing a 6 Degrees-of-Freedom (DOF) dynamic and kinematic control system for a single AUV within a cooperation framework system that will enhance the divers' capabilities and/or reduce associated risks with diving operations*.

The paper is organized as follows. The problem addressed in the paper is expanded in Section II. Section III refers to possible cooperation frameworks in various diving operations. Section IV expands state of the art solutions towards locating and tracking a diver, wrapping up with an architecture proposal towards designing the AUV control system, presented in Section V. Simulation results are presented in Section VI and Section VII summarizes the main conclusions of the paper.

A. Mathematical Notation

Throughout the paper we used bold symbols and letter to denote vectors or matrices and normal script for scalar. Vectors and matrices are represented in lower and upper case, respectively. The symbol $\mathbf{I}_n$ denotes an $n \times n$ identity matrix. The mapping $\mathbf{S}(\cdot) : \mathbb{R}^3 \mapsto \mathcal{S}$ denotes the skew-symmetric operator, i.e $\mathbf{S}(\mathbf{a})\mathbf{b} = \mathbf{a} \times \mathbf{b}$, where $\mathbf{a}, \mathbf{b} \in \mathbb{R}^3$ and $\times$ is the vector cross product. The asymptotic and supremum norm are denoted by $\lim_{t\to\infty} \|\mathbf{x(t)}\|$ and $\|\mathbf{x}\|_\infty = \sup_{t\geq 0} \|\mathbf{x}(t)\|$, respectively. For simplicity of notation, except when explicitly stated, $\|\cdot\|$ denotes the Euclidean 2-norm. For an arbitrary $n \times m$ matrix $\mathbf{A}$, if the p-norm for vectors is used, the corresponding (induced) norm is defined as $\|\mathbf{A}\|_p = \sup_{\mathbf{x}\neq\mathbf{0}} \frac{\|\mathbf{Ax}\|_p}{\|\mathbf{x}_p\|}, \forall \mathbf{x} \in \mathbb{R}^n$.

II. PROBLEM STATEMENT

The present article tackles the problem of enabling cooperating behaviours between a diver and an AUV through the

This work was supported by FCT through project H2020 EU Marine Robotics Research Infrastructure Network (Project ID 731103) and the Blue Roses project [863619], co-funded by the European Maritime and Fisheries fund of the European Union.

design of an autonomous control and navigation system, both from a theoretical and practical point of view.

A. Diver-AUV Cooperation

The problem of cooperation between an AUV and a diver can be formulated in various ways, and there is no optimal approach as there exists different types of diving operations, each with respective risks and tasks. It is imperative to first identify the mission at hand and then proceed to formulate the possible cooperation strategies.

B. Diver Tracking

Gathering information about the diver whereabouts in underwater environments is beneficial for vehicle guidance, control and navigation systems. This can formulated in a two-fold problem approach: i) *target localization*; ii) *target tracking*. The former concerns the estimation of a target position, e.g, diver, object, robot, dock, animal, via measurements accessed by an agent from a suite of sensors. The latter, through solving this localization problem and obtaining estimates of the target position, addresses the problem of obtaining additional information about other kinematic components of the target state, e.g., velocity, acceleration, etc. This paper focuses on solving the localization (and tracking) problem of estimating linear motion quantities of a target, that is, the target is assumed to have no intrinsic attitude and, consequently, no associated angular velocity. We instead interpret the target attitude/angular velocity to be associated with the mission requirements, which is then provided by a guidance system.

C. AUV Motion Control

Assuming we have a functional vehicle navigation system, with the means to locate and track a diver and determine the AUV pose as well as velocity, we address the control problem of designing a 6 DOF dynamic and kinematic controller for a single fully-actuated AUV under the proposed cooperation architecture.

III. Diver-AUV Underwater Cooperation

While the concept of cooperation is not new in the world of robotics, only recent development in the areas of underwater communication, navigation and electronics [18] have allowed for such strategies to be carried out in the challenging marine environment. Specific to cooperation is the concept of diver-AUV cooperation which concerns the different ways an AUV can cooperate with the diver to help enhance the tasks' feasibility and/or reduce the associated risks faced by the diver. Possible cooperation strategies were identified, such as: (i) follow the diver within a safety radius, allowing different tasks to be performed such as, pointing towards the desired location underwater to aid the diver navigation, or carrying certain tools/equipment; (ii) observe the diver in the surrounding area, in a station-keeping manoeuvre to provide light or other improvements to the working area; (iii) Monitor the diver and check their vital signs, reducing potential diving associated risks; (iv) Dynamically plan the robot mission on-line via gesture or other communication interfaces with the diver. Common risks associated with diving operations include low visibility, decompression sickness, nitrogen narcosis, currents and a general lack of orientation. Other risks may arise, but it depends on the diving operation at hand, so an initial brief review and discussion are held to contextualize our problem, highlighting the specific risks/challenges and benefits towards implementing such cooperation strategies.

Commercial/Industrial Diving: These concern the engineering work performed in underwater environments such as building, repair, examination, or maintenance In commercial diving, common risks are associated with the surrounding hazardous working environments and the use of specialized equipment. By implementing some cooperation strategies between a diver and an AUV, the diver fatigue can be reduced during diving, the diver could have a safer and faster approach towards the worksite, or have a helping hand from the robot in hard-to-operate tools, e.g., valves, levers, with recent work done towards this latter approach [19].

Scientific Diving: These diving operations have their purpose built on the pursuit of knowledge and research development related to science, with tasks performed underwater being of a scientific nature [20]. Common challenges in these missions are associated with not knowing the location of potential objects or areas of interest (e.g., underwater archaeology) or ruining data (e.g., marine biology). These cooperation strategies could benefit the mission development, allowing a quicker and safer delivery of material of interest to the surface, a better site inspection or finding new areas of interest.

Media Diving: Media diving operations specialize in underwater cinematography and photography, related to oceanography, engineering, cinema and television industry. Divers often use specialized equipment (e.g., video cameras, underwater lighting). There is almost no need to navigate accurately and know the whereabouts of the environment as they usually accompany other divers/objects. Relative to cooperation strategies, automation behaviours have been proven to benefit filming operations [21], with steadier recording, self-recording and transportation of certain apparatus.

Military Diving: Military diving operations concern the tasks performed by military personnel in underwater environments. These can involve more risks due to the military nature of these operations, lack of time to prepare and plan But, contrary to popular belief, accidents are less likely to happen during these types of diving operations compared to recreational diving, as pointed out by the Poland Military Institute of Medicine [22]. AUVs can support the diver towards search-and-rescue missions via acoustic or visual technology, and safely dispose of found hazardous material.

A. Proposed Cooperation Architecture

Given this discussion, we propose a general-purpose architecture, presented in Fig. 1, promoting some cooperation strategies mentioned above and serving as a basis of development and motivation for the control system derived afterwards. Under this architecture, we then desire the AUV to: (R1) follow and accompany the diver during diving operations, maintaining a safe distance; (R2) Position itself, in any given desired location according to mission requirements; (R3) Orient itself accordingly, independently of position, according to mission requirements.

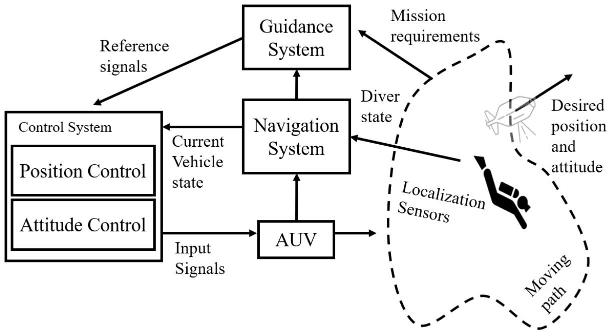

Fig. 1. An overview of the cooperation strategy implemented in this thesis, formulated in this architecture diagram.

Under this cooperation architecture, the AUV possesses a capable navigation system towards estimating its position and velocity, and a guidance system that takes the information from the mission requirements, diver position and velocity to produce the necessary reference signals for the control system. This diver state will be obtained by solving the target localization and tracking problem, via the vehicle onboard sensors.

IV. Tracking a Diver

Much research has been devoted to solving the tracking problem, from aerial to marine environments, with the predominant paradigm of using a stochastic estimation approach [3], [4], [23]. These can range from simple Kalman filters and their variants of extended/unscented Kalman filters, or even particle filters. Our main focus is not on the tracking solution of an arbitrary target, but of divers which typically move through the water at a low velocity and without abrupt motion changes. Therefore, we focus our approach on the Kalman filter solution, as it is a well known reliable and simple solution in the literature. These will allow paying more detailed attention to the actual procedure towards the design and implementation of the filter under these diver-AUV cooperation circumstances.

A. Process and Measurement Model

For filtering purposes, since we adopt a Kalman approach, the discrete process model and the measurement model of the diver are described by a linear time-invariant state-space discrete system driven by white process and measurement noise, $\boldsymbol{w}_k$ and $\boldsymbol{v}_k$ respectively, represented as additive white Gaussian noise, with zero mean and time-invariant covariance matrix $\boldsymbol{Q}$ and $\boldsymbol{R}$

$$\boldsymbol{x}_k = \boldsymbol{\Phi}\boldsymbol{x}_{k-1} + \boldsymbol{w}_k, \tag{1}$$

$$\boldsymbol{z}_k = \boldsymbol{H}\boldsymbol{x}_k + \boldsymbol{v}_k, \tag{2}$$

where $\boldsymbol{\Phi} \in \mathbb{M}(n,n)$ denotes the transition $n \times n$ matrix from state $\boldsymbol{x} \in \mathbb{R}^n$ at time k to $(k+1)$, with $\mathbb{M}(n,m)$ representing the space of $n \times m$ real valued matrices, and $\boldsymbol{H} \in \mathbb{M}(m,n)$ denotes the measurement matrix that yields the measurement $\boldsymbol{z} \in \mathbb{R}^m$ taken at time k with the target at a given state $\boldsymbol{x}_k$, where $k,m,n \in \mathbb{N}$. Our state vector assumes the target linear motion quantities, i.e position and velocity, defined as $\boldsymbol{x} = [\boldsymbol{p}_t^T, \boldsymbol{v}_t^T]^T \in \mathbb{R}^6$, where $\boldsymbol{p}_t \in \mathbb{R}^3$ and $\boldsymbol{v}_t \in \mathbb{R}^3$ denote the target's inertial position and body velocity.

Relative to the structures of the transition matrix $\boldsymbol{\Phi}$, tracking Kalman based filter structures used for underwater target tracking is usually similar, with some having slight differences [3]. There are three frequently used target motion models: the constant velocity (CV) model, the constant acceleration (CA) model and the turning model. The most popular and common approach [23] is to consider the target dynamics with having a constant velocity (CV) between each sampling time. Empirically, this is compatible with the movement that a diver performs underwater whose movements are smooth, with almost non-existent acceleration, and do not change direction rapidly.. With this, assuming a constant velocity (CV) target model the transition matrix structure takes the following form

$$\boldsymbol{\Phi} = \begin{bmatrix} 1 & 0 & 0 & T_s & 0 & 0 \\ 0 & 1 & 0 & 0 & T_s & 0 \\ 0 & 0 & 1 & 0 & 0 & T_s \\ 0 & 0 & 0 & 1 & 0 & 0 \\ 0 & 0 & 0 & 0 & 1 & 0 \\ 0 & 0 & 0 & 0 & 0 & 1 \end{bmatrix}, \tag{3}$$

where $T_s \in \mathbb{R}$ denotes the sampling time interval.

The structure of the measurement model $\boldsymbol{H}$, since we are dealing with a second-order system, we consider a measurement model structure regarding position-only (POM). We do not discuss a position-velocity-measurement (PVM) approach as it is not common for underwater sensors to measure a target velocity. It is fair to assume that we only have measures of a target position, therefore our measurement matrix takes the following structure

$$\boldsymbol{H} = \begin{bmatrix} 1 & 0 & 0 & 0 & 0 & 0 \\ 0 & 1 & 0 & 0 & 0 & 0 \\ 0 & 0 & 1 & 0 & 0 & 0 \end{bmatrix}. \tag{4}$$

B. A Kalman Filter Solution

The Kalman filter algorithm based on these models recursively estimates the state vectors in a mean-square sense via the Kalman filter equations of prediction and estimation, respectively given by

$$\tilde{\boldsymbol{x}}_k = \boldsymbol{\Phi}\hat{\boldsymbol{x}}_{k-1}, \tag{5}$$

$$\hat{\boldsymbol{x}}_k = \tilde{\boldsymbol{x}}_k + \boldsymbol{K}_k(\boldsymbol{z}_k - \boldsymbol{H}\tilde{\boldsymbol{x}}_k), \tag{6}$$

where the parameter $\boldsymbol{K}_k$ denotes the Kalman gain that minimizes the steady-state expected value of the error covariance, given by $\lim_{t\to\infty} E[(\boldsymbol{x}_k - \hat{\boldsymbol{x}}_k)(\boldsymbol{x}_k - \hat{\boldsymbol{x}}_k)^T]$, following the standard Kalman practice of solving the Ricatti equation.

C. Filter Parameter Design

The next step is to design the parameters of the filter that relate to the noise effect on the system state and sensor measurements. It is not known a general approach to this problem [24] but in conventional tracking systems, a common model of process noise design is the *random acceleration* (RA) model [24], with the covariance matrix taking the following structure

$$
\boldsymbol{Q} = \begin{bmatrix} T_s^2/4 & 0 & 0 & T_s/2 & 0 & 0 \\ 0 & T_s^2/4 & 0 & 0 & T_s/2 & 0 \\ 0 & 0 & T_s^2/4 & 0 & 0 & T_s/2 \\ T_s/2 & 0 & 0 & 1 & 0 & 0 \\ 0 & T_s/2 & 0 & 0 & 1 & 0 \\ 0 & 0 & T_s/2 & 0 & 0 & 1 \end{bmatrix} \sigma_q^2 T_s^2. \tag{7}
$$

We can view σ_q as the standard deviation of a Gaussian sequence that models the target acceleration $\boldsymbol{w}_q$, assumed to be constant during the sampling interval T_s, a common practice in the literature [10], [24]..

Relative to the measurement covariance matrix $\boldsymbol{R}$, this is a representative parameter of the sensing equipment accuracy, usually estimated from analyzing their specifications. We will adopt a simple solution consisting of the sensor's data variance of the position measurement errors since our filter adopts a POM approach, Following the approach of the authors in [24] the measurement covariance matrix takes the following form

$$
\boldsymbol{R} = \begin{bmatrix} \sigma_x & 0 & 0 \\ 0 & \sigma_y & 0 \\ 0 & 0 & \sigma_z \end{bmatrix}, \tag{8}
$$

where σ_x, σ_y and σ_z denote the variance of position measurements' errors in the horizontal (x and y) and vertical axis (z).

D. Diver Localization

Having defined the solution towards the tracking problem, we now move towards solving the challenging problem of localization in the context of tracking the diver via measurements of their position.

LBL/SBL Systems: A customary approach towards the localization of targets is the use of fixed beacons via principles of triangulation and clock synchronization. These acoustic beacons (transducers) are fixed in some known location and can either be *long baseline* (LBL) and *short baseline* (SBL) acoustic positioning systems. The difference lies in distances (baselines) between these beacons, the former usually fixated in the seabed or buoys separated by long distances between each transducer, and the latter on a vessel or another platform of choice, with only meters separating each transducer. LBL systems are well known and robust solutions towards locating a target [18] providing an alternative solution to GNSS, or inertial based navigation systems. However, they can be difficult to implement due to the need for physical beacons with the known position being built on-site - sometimes unfeasible for divers to fixate such beacons. On the other hand, SBL systems surge as a mobile alternative, being easier to deploy and operate, favoured for research operations centred around a host vessel [25]. The accuracy of the estimate is largely dependent on the length of the baseline and may require the agents to operate in the close vicinity of the ship or platform of choice, translating in a lesser range of operation compared to LBL systems [26]. However, both LBL and SBL suffer the problem of complex infrastructure and require extra agents at play to estimate the target position.

USBL Systems: Another approach, similar to LBL and SBL systems, is the *ultra-short baseline* (USBL) acoustic positioning system. It is a ranging mechanism composed of a small array of transducers, equally distanced, usually with a baseline on the order of centimetres, that computes the position of a target based on the travel time of acoustic signals emitted by the transponder [27]. This small configuration, depicted in Fig. 2, allows an easy implementation on a singular mobile platform, such as an AUV.

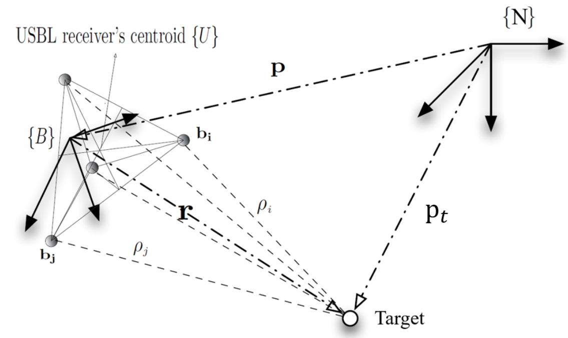

Fig. 2. An USBL system with i receivers, with a representation of the sensor frame $\{U\}$ centroid, the body-fixed frame $\{B\}$ attached to the moving platform (e.g, AUV), and an inertial frame $\{N\}$ (adapted from [5]).

They work under the principle of planar approximation of acoustic waves, implying that in close-range operations with the target, estimation error increases. It is considered to yield satisfactory results at distances approximately 10 times larger than the baseline of the receiving array [5]. Additionally, if the vehicle pose is known, it is possible to know the target inertial position. These systems are quite portable and do not require additional beacons spread through the environments or in other agents. However, their positioning accuracy is not as good compared to LBL/SBL systems [18], and require huge precision to maintain the transducers equally distanced from each other. Furthermore, these systems suffer from blind-spot regions, with certain azimuth and elevation angles that are "blind" to the target.

Visual Based Localization: Another strategy used towards localization of targets is via the use of optical sensors or acoustic imaging sensors. These can provide additional information about the surrounding environment that are not accessible using traditional acoustic sensors. This field is relatively new in the Marine Robotics literature due to the recent increase in onboard computing power and advances in image processing techniques. Common approaches using optical sensors are based on detecting a target based on visual data, processing the data and proceeding to maintain a visual reference [28]. These systems do not scale well with distance, can have a limited field of views (depending on the optical sensor) and in poor-visibility conditions, the performance is drastically reduced. Acoustic imaging sensors provide a robust alternative as acoustic propagation is more suited in marine environments. Standard procedure passes through obtaining an image from an acoustic sensor and implementing image processing or computer vision techniques towards interpreting the data, obtaining a location of the diver in the visual frame and then tracking it [29]. But these acoustic sensors can be more complex, costly and power-hungry compared to optical sensors, do not possess a high resolution and can suffer from scattering issues due to multi-path propagation of acoustic waves in underwater scenarios [18].

Single Range Measurements: The concept of single range localization, roughly speaking, considers an agent that has access to single range measurements to a target, from a set of onboard sensors and aims to estimate the position of the target. This strategy has been the subject of recent interest as a cost-efficient solution with relatively easy implementation, with current available underwater acoustics technology. The principle behinds this concept, as shown in Fig. 3, considers that, via certain excitation conditions (e.g, agent motion), it is possible to design an observable filter that estimates the position of the target, satisfying certain stability criteria for the estimation error dynamics [6]. These solutions can also be extended to multiple agents, relaxing the necessary constraints to observe the target, allowing for different motions to be performed by different agents (e.g., straight lines, cycloid-type, etc) [30]. However, these suffer from a huge drawback of constraining the vehicle motion to be specific otherwise the target becomes "unobservable".

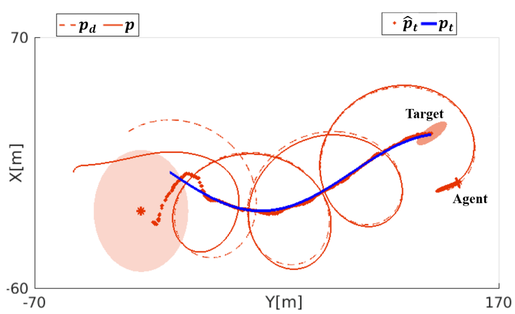

Fig. 3. An AUV (with trajectory represented in red, with true and desired position $\boldsymbol{p}$ and $\boldsymbol{p}_d$, respectively) performs a circular motion around a target (represented in blue, with true and estimated position $\boldsymbol{p}_t$ and $\hat{\boldsymbol{p}}_t$, respectively) to obtain reliable estimates of its position (adapted from [30]).

V. AUV Nonlinear Controller Design

This section proposes a nonlinear control law under the proposed architecture to regulate the motion of an AUV to follow a prescribed path (R1), position itself at any point in this path (R2) and stabilize its attitude at an arbitrary reference point (R3), in the presence of a constant unknown ocean current disturbance. The kinematic and dynamic model of an underwater vehicle moving in a three-dimensional space is first derived and then proceed to derive the control law at a kinematic and dynamic level. It is assumed that the AUV inertial position $\boldsymbol{p} \in \mathbb{R}^3$, attitude $\boldsymbol{R}_v \in SO(3)$ and velocity $\boldsymbol{\nu} = [\boldsymbol{v}, \boldsymbol{\omega}]^T \in \mathbb{R}^6$ is known, where $\boldsymbol{v} \in \mathbb{R}^3$ and $\boldsymbol{\omega} \in \mathbb{R}^3$ denotes the AUV linear and angular velocity, respectively, provided by a navigation system. It is also assumed that the diver inertial position $\boldsymbol{p}_t \in \mathbb{R}^3$ and linear velocity $\boldsymbol{v}_t \in \mathbb{R}^3$ is known, provided by a target tracking filter. The diver attitude $\boldsymbol{R}_t \in SO(3)$ and angular velocity $\boldsymbol{\omega}_t \in \mathbb{R}^3$is provided by a guidance system, as these components are not measured but instead defined depending on the mission requirements.

A. Vehicle Modeling

Following standard practise and notation in marine craft literature [31], the general kinematic and dynamic equations of motion of the vehicle in three dimensions can be developed using an inertial coordinate frame $\{N\}$ and a body-fixed coordinate frame $\{B\}$ attached to the centre of mass of the AUV. Considering an irrotational ocean current with inertial velocity $\boldsymbol{V}_c = [\boldsymbol{V}_{c_v}, \boldsymbol{0}]^T \in \mathbb{R}^6$ the 6 DOF kinematic equations of motion of an underwater vehicle for linear and angular motion can be expressed as

$$\dot{\boldsymbol{p}} = \boldsymbol{R}_v \boldsymbol{v}_r + \boldsymbol{V}_{c_v}, \tag{9a}$$

$$\dot{\boldsymbol{R}}_v = \boldsymbol{S}(\boldsymbol{\omega}) \boldsymbol{R}_v, \tag{9b}$$

where $\boldsymbol{v}_r = \boldsymbol{v} - \boldsymbol{V}_{c_v}$ are the body axis components of the vehicle's linear velocity with respect to the water.

Considering that an underwater vehicle motion through water is subject to external forces and possesses actuation capabilities, the 6 DOF equations of motion take the vector form

$$\boldsymbol{M}\dot{\boldsymbol{\nu}}_r + \boldsymbol{C}(\boldsymbol{\nu}_r)\boldsymbol{\nu}_r + \boldsymbol{D}(\boldsymbol{\nu}_r)\boldsymbol{\nu}_r = \boldsymbol{\tau}, \tag{10}$$

where $\boldsymbol{\nu}_r = [\boldsymbol{v}_r, \boldsymbol{\omega}]^T$ represents the vehicle linear and angular velocity w.r.t to the water, $\boldsymbol{M} \in \mathbb{M}(6,6)$ denotes the matrix of rigid-body inertia and added mass terms, $\boldsymbol{C}(\boldsymbol{\nu}_r) \in \mathbb{M}(6,6)$ is the matrix of rigid-body and added mass Coriolis and centripetal terms, $\boldsymbol{D}(\boldsymbol{\nu}_r) \in \mathbb{M}(6,6)$ represents the matrix of linear and nonlinear hydrodynamic damping terms, and $\boldsymbol{\tau} \in \mathbb{R}^6$ is a vector of forces and moments generated from the vehicle actuators.

B. Position and Attitude Control

Central to the inner-outer loop control design, the outer loop acts on a kinematic level of the vehicle motion. Considering that our vehicle is fully-actuated, at a kinematic level the control objective consists of recruiting the linear and angular relative velocities $\boldsymbol{v}_r$ and $\boldsymbol{\omega}_r$ respectively, to solve a two-fold problem: 1) regulate the vehicle position to follow a path and meet the desired position in this path; 2) regulate the vehicle attitude to achieve an arbitrary reference. At this stage, it is assumed that the ocean current linear velocity $\boldsymbol{V}_{c_v}$ is known.

For the former problem of controlling the vehicle position, illustrated in Fig. 4, we consider an *a priori* specified path expressed to a moving target, that is a parametric closed $\mathcal{C}^2$ continuous curve. This path is parameterized by continuous variable $\gamma \in \mathbb{R}$, whose derivative $\dot{\gamma}$ is an extra input control parameter. Let the virtual point $\boldsymbol{p}_d^t(\gamma) \in \mathbb{R}^3$ denote the position of the virtual reference point for the vehicle to follow, expressed in a target frame $\{T\}$ whose origin is attached to the target position $\boldsymbol{p}_t$. To obtain its inertial position and velocity, we can express its virtual position for a given γ, as follows

$$\boldsymbol{p}_d(\gamma) = \boldsymbol{p}_t + \boldsymbol{R}_t \boldsymbol{p}_d^t(\gamma), \tag{11}$$

$$\dot{\boldsymbol{p}_d}(\gamma) = \boldsymbol{v}_t + \boldsymbol{R}_t \left(\frac{\partial \boldsymbol{p}_d^t(\gamma)}{\partial \gamma} \dot{\gamma} + \boldsymbol{S}(\boldsymbol{w}_t) \boldsymbol{p}_d^t(\gamma) \right). \tag{12}$$

With this, we can formulate the following *moving path-following* problem, as follows:

Problem 1. *Consider an AUV with kinematics equation given by* (9a) *and* (9b). *Let* $\boldsymbol{p}_d^t(\gamma)$ *be sufficiently smooth and its derivatives with respect to* γ *are bounded. Derive a control law for* $\boldsymbol{v}_r$ *and* $\dot{\gamma}$ *such that i) the position of the vehicle* $\boldsymbol{p}$ *converges to* $\boldsymbol{p}_d(\gamma)$*, i.e., the positioning error* $\boldsymbol{p} - \boldsymbol{p}_d$ *has a globally asymptotically stable (GAS) equilibrium point at the origin and ii) the path parameterization variable* γ *converges to* γ_d*, i.e, the virtual particle position error* $\gamma - \gamma_d$ *has a globally asymptotically stable (GAS) equilibrium point at the origin.*

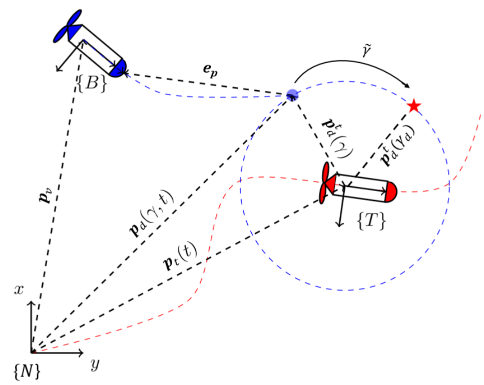

Fig. 4. Representation of the *moving path-following* problem, where our vehicle is represented in blue, and an arbitrary target is represented in red, e.g, a diver, other vehicle, etc (adapted from [10]).

The error associated with the vehicle and the desired position is re-defined in the body-fixed frame as follows, with respective dynamics

$$\boldsymbol{e}_p = \boldsymbol{R}_v^T(\boldsymbol{p} - \boldsymbol{p}_d), \tag{13}$$

$$\dot{\boldsymbol{e}}_p = -\boldsymbol{S}(\boldsymbol{\omega}_r)\boldsymbol{e}_p + \boldsymbol{v}_r + \\ + \boldsymbol{R}_v^T\left(\boldsymbol{V}_{c_v} - \boldsymbol{v}_t - \boldsymbol{R}_t\left(\frac{\partial \boldsymbol{p}_d^t(\gamma)}{\partial\gamma}\dot{\gamma} + \boldsymbol{S}(\boldsymbol{w}_t)\boldsymbol{p}_d^t(\gamma)\right)\right). \tag{14}$$

The path position error and respective dynamics are, respectively, given by

$$\tilde{\gamma} = \gamma - \gamma_d, \tag{15a}$$

$$\dot{\tilde{\gamma}} = \dot{\gamma} - \dot{\gamma}_d. \tag{15b}$$

The following control law is proposed to solve Problem 1, as follows:

We define a saturation function according to the following definition:

Proposition 1. *Consider the system described in* (9a) *in closed-loop with the control laws*

$$\boldsymbol{v}_d = -\lambda_p\boldsymbol{\sigma}\left(\frac{k_p}{\lambda_p}\boldsymbol{e}_p\right) - \\ - \boldsymbol{R}_v^T\left(\boldsymbol{V}_{c_v} - \boldsymbol{v}_t - \boldsymbol{R}_t\left(\frac{\partial \boldsymbol{p}_d^t(\gamma)}{\partial\gamma}\dot{\gamma}_d + \boldsymbol{S}(\boldsymbol{w}_t)\boldsymbol{p}_d^t(\gamma)\right)\right), \tag{16}$$

$$\dot{\gamma} = \dot{\gamma}_d - k_\gamma\left(\rho_{\tilde{\gamma}}\sigma(k_{\tilde{\gamma}}\tilde{\gamma}) - \boldsymbol{e}_p^T\boldsymbol{R}_v^T\boldsymbol{R}_t^n\frac{\partial p_d^t(\gamma)}{\partial\gamma}\right), \tag{17}$$

where $\boldsymbol{\sigma}$ *represents a saturation function [32, Appendix C.1], and it is assumed that* $\boldsymbol{v}_d = \boldsymbol{v}_r$ *at a kinematic level. Additionally,* $\rho_{\tilde{\gamma}}$ *and* $k_{\tilde{\gamma}}$ *are positive parameter gains, and* k_γ*,* λ_p *and* k_p *are positive controller gains. Then, the origin of positioning error system* $\boldsymbol{e}_p = \boldsymbol{0}$ *and path parameterization position error system* $\tilde{\gamma} = 0$ *are GAS.*

Proof. Define the following Lyapunov candidate

$$V_p(\tilde{\gamma}, \boldsymbol{e}_p) = \frac{1}{2}\boldsymbol{e}_p^T\boldsymbol{e}_p + \frac{\rho_{\tilde{\gamma}}}{k_{\tilde{\gamma}}}\int_0^{\tilde{\gamma}}\sigma(k_{\tilde{\gamma}}s)\,ds > 0, \tag{18}$$

for every $\boldsymbol{e}_p \in \mathbb{R}^3\backslash\{\boldsymbol{0}\}$ and $\tilde{\gamma} \in \mathbb{R}\backslash\{0\}$. The time derivative of (18) and using the error dynamics (14) and (15b) is given by

$$\dot{V}_p = \boldsymbol{e}_p^T\left(\boldsymbol{v}_r + \boldsymbol{R}_v^T\left(\boldsymbol{V}_{c_v} - \boldsymbol{v}_t - \boldsymbol{R}_t\left(\frac{\partial \boldsymbol{p}_d^t(\gamma)}{\partial\gamma}\dot{\gamma}_d + \right.\right.\right. \\ \left.\left.\left. + \boldsymbol{S}(\boldsymbol{w}_t)\boldsymbol{p}_d^t(\gamma)\right)\right)\right) + \dot{\tilde{\gamma}}\left(\rho_{\tilde{\gamma}}\sigma(k_{\tilde{\gamma}}\tilde{\gamma}) - \boldsymbol{e}^T\boldsymbol{R}_v^T\boldsymbol{R}_t^n\frac{\partial \boldsymbol{p}_d^t(\gamma)}{\partial\gamma}\right). \tag{19}$$

Substituting the control law (16)-(17) in (19) yields

$$\dot{V}_p = -\boldsymbol{e}_p^T\lambda_p\boldsymbol{\sigma}\left(\frac{k_p}{\lambda_p}\boldsymbol{e}_p\right) - \\ - k_\gamma\left(\rho_{\tilde{\gamma}}\sigma(k_{\tilde{\gamma}}\tilde{\gamma}) - \boldsymbol{e}^T\boldsymbol{R}_v^T\boldsymbol{R}_t^n\frac{\partial p_d^t(\gamma)}{\partial\gamma}\right)^2, \tag{20}$$

making $\dot{V}_p$ negative definite. Since $V_p(0,0) = 0$ and $V_p(\tilde{\gamma}, \boldsymbol{e}_p) \Rightarrow \infty$ when $\|\boldsymbol{e}_p\|, \|\tilde{\gamma}\| \Rightarrow \infty$ is GAS. □

Having solved the former position control problem, we now focus on the latter problem of regulating the vehicle attitude to meet an arbitrary reference. In broad terms, the problem at hand consists of controlling the vehicle body frame $\{B\}$ with an associated rotation $\boldsymbol{R}_v$ and ensuring convergence to the desired frame $\{D\}$ with respective rotation matrix $\boldsymbol{R}_d$, where both frame with respect to the inertial frame $\{N\}$. Additionally, suppose there exist a matrix $\boldsymbol{Q}$ such that it satisfies the following assumption:

Assumption 1. *The matrix* $\boldsymbol{Q} \in \mathbb{M}(3, m)$ *with* $m > 0$ *is such that the singular values are all distinct.*

As pointed out by the author [33], this can be interpreted as an observability condition. Then, we can formulate the following *attitude set-point regulation* problem, as follows:

Problem 2. *Consider an AUV with rotational kinematics equation given by 9b. Let* $\boldsymbol{R}_d(\boldsymbol{\Theta}_d)$ *be a target rotation matrix, parameterized by a fixed reference, defined a priori, via* $\boldsymbol{\Theta}_d = [\phi_d, \theta_d, \psi_d]^T$*. Additionally suppose that there exists a matrix* $\boldsymbol{Q}$ *that satisfies Assumption 1. Derive a feedback control for* $\boldsymbol{\omega}_r$ *such that the body frame rotation matrix* $\boldsymbol{R}_v$ *converges to* $\boldsymbol{R}_d$*, i.e, the rotational error* $\boldsymbol{R}_v^T\boldsymbol{R}_d$ *has an almost globally asymptotically stable (AGAS) equilibrium point at* $\boldsymbol{I}_3$*, where* $\boldsymbol{I}_3$ *is the identity matrix in three dimensions.*

For this purpose, define the error rotation matrix, with the respective dynamics, as follows

$$\boldsymbol{R}_e = \boldsymbol{R}_b^{n^T} \boldsymbol{R}_d, \tag{21}$$

$$\dot{\boldsymbol{R}}_e = -\boldsymbol{S}(\boldsymbol{\omega}_r)\boldsymbol{R}_e. \tag{22}$$

Following the strategy of the authors in [11], it is convenient to express the error as a function on $SO(3)$, as follows

$$e_\Theta(\boldsymbol{R}_e) = \text{Tr}\left((\boldsymbol{I}_3 - \boldsymbol{R}_e)\,\boldsymbol{Q}\boldsymbol{Q}^T\right), \tag{23}$$

where $\text{Tr}(\cdot)$ denotes the trace of a square matrix, defined as the sum of all elements in the matrix diagonal. If the assumption made regarding matrix $\boldsymbol{Q}$ holds, the error function e_Θ is a positive definite Morse function i.e, it is a function with nondegenerate isolated critical points [34] with a global minimum at $\boldsymbol{R}_e = \boldsymbol{I}_3$, a maximum and two saddle points. Computing the time derivative, we have

$$\dot{e}_\Theta(\boldsymbol{R}_e) = -\boldsymbol{S}^{-1}(\boldsymbol{R}_e\boldsymbol{Q}\boldsymbol{Q}^T - \boldsymbol{Q}\boldsymbol{Q}^T\boldsymbol{R}_e^T)^T\boldsymbol{\omega}_r, \tag{24}$$

where $\boldsymbol{S}^{-1} : SO(3) \mapsto \mathbb{R}^3$ corresponds to the inverse mapping of the cross-product operator.

With this, the following control law is proposed to solve Problem 2, as follows:

Proposition 2. *Consider the system given by* (9b) *and the following control law in closed-loop*

$$\boldsymbol{\omega}_d = \boldsymbol{K}_\omega \boldsymbol{S}^{-1}(\boldsymbol{R}_e\boldsymbol{Q}\boldsymbol{Q}^T - \boldsymbol{Q}\boldsymbol{Q}^T\boldsymbol{R}_e^T), \tag{25}$$

where $\boldsymbol{K}_\omega$ is a positive definite gain matrix, and it is assumed that $\boldsymbol{\omega}_d = \boldsymbol{\omega}_r$ at a kinematic level. Then, the equilibrium point of the error rotation matrix $R_e = \boldsymbol{I}_3$ is AGAS. Moreover, there exists a neighborhood of $\boldsymbol{R}_e = \boldsymbol{I}_3$, such that all solutions starting inside it converge exponentially fast to $\boldsymbol{R}_e = \boldsymbol{I}_3$.

The proof will follow a similar approach as done by the authors in [11], disregarding the vehicle translation kinematics and dynamics. Define a Lyapunov candidate for the vehicle error rotation matrix, as follows

$$V_\Theta(\boldsymbol{R}_e) = e_\Theta(\boldsymbol{R}_e) = \text{Tr}\left((\boldsymbol{I}_3 - \boldsymbol{R}_e)\,\boldsymbol{Q}\boldsymbol{Q}^T\right). \tag{26}$$

Taking the time derivative of (26) and using the attitude error dynamics (24) in closed-loop with the control law (25), we have

$$\dot{V}_\Theta = -\boldsymbol{S}^{-1}(\boldsymbol{R}_e\boldsymbol{Q}\boldsymbol{Q}^T - \boldsymbol{Q}\boldsymbol{Q}^T\boldsymbol{R}_e^T)^T\boldsymbol{K}_\omega\boldsymbol{S}^{-1}(\boldsymbol{R}_e\boldsymbol{Q}\boldsymbol{Q}^T - \boldsymbol{Q}\boldsymbol{Q}^T\boldsymbol{R}_e^T). \tag{27}$$

It follows immediately that $\dot{V}_\Theta$ is negative semi-definite. We have that the largest invariant set $\mathcal{M} = \{\boldsymbol{R}_e \in SO(3) \mid \dot{V}_\Theta = 0\}$ is the set of points $\boldsymbol{R}_e$ that are critical points of V_Θ, which are the global minimum $\boldsymbol{R}_e = \boldsymbol{I}_3$, a maximum and two saddle points. Applying LaSalle's invariance principle, we conclude that the closed-loop trajectories of the error system (24) converge to $\mathcal{M}$ as $t \to \infty$. Additionally, the authors in [11] prove that except for the point $\boldsymbol{R}_e = \boldsymbol{I}_3$ all equilibrium points $\boldsymbol{R}_e = \boldsymbol{R}_c \in \mathcal{M}$ have an unstable manifold. In loose terms, this prevent trajectories remaining in this manifold, allowing them to asymptotically converge to the desired equilibrium. However, it may happen that the convergence to the equilibrium can be affected near this *thin* set [11]. With this, the equilibrium point $\boldsymbol{R}_e = \boldsymbol{I}_3$ is proven to be AGAS.

C. AUV Dynamics Control

Now, having defined the position and attitude control laws for the outer loop controller, we proceed to derive an inner loop whose task is to meet the desired velocity assignments by inverting the plant dynamics, in this case, our AUV nonlinear dynamics. With this, the following control problem is formulated:

Problem 3. *Consider the 6 DOF dynamical model of the vehicle given by* (10). *Let $\boldsymbol{\nu}_d = [\boldsymbol{v}_d, \boldsymbol{\omega}_d]^T \in \mathbb{R}^6$ be a desired speed requirement from the outer loop, and suppose that $\boldsymbol{\nu}_d$ is sufficiently smooth and its derivative is bounded. Derive a feedback control law $\boldsymbol{\tau}$ such that the relative velocity error $\boldsymbol{\nu}_r - \boldsymbol{\nu}_d$ has a globally exponentially stable (GES) equilibrium point at the origin.*

For this purpose, we first define the error $\boldsymbol{e}_d = \boldsymbol{\nu}_r - \boldsymbol{\nu}_d \in \mathbb{R}^3$. With this. we can rewrite the AUV equations of motion in error form, as follows

$$\boldsymbol{M}\dot{\boldsymbol{e}}_d = \boldsymbol{\tau} - \boldsymbol{M}\dot{\boldsymbol{\nu}}_d - \boldsymbol{C}(\boldsymbol{\nu}_r)\boldsymbol{\nu}_r - \boldsymbol{D}(\boldsymbol{\nu}_r)\boldsymbol{\nu}_d - \boldsymbol{D}(\boldsymbol{\nu}_r)\boldsymbol{e}_d. \tag{28}$$

Then, the following inner loop control law is proposed:

Proposition 3. *Consider the system described by* (28) *and the following control law in closed-loop*

$$\boldsymbol{\tau} = -\boldsymbol{K}_d\boldsymbol{e}_d + \boldsymbol{M}\dot{\boldsymbol{\nu}}_d + \boldsymbol{D}(\boldsymbol{\nu}_r)\boldsymbol{\nu}_d + \boldsymbol{C}(\boldsymbol{\nu}_r)\boldsymbol{\nu}_r, \tag{29}$$

where $\boldsymbol{K}_d$ is a positive definite gain matrix. Then, the origin of the velocity error system $\boldsymbol{e}_d = \boldsymbol{0}$ has a GES equilibrium point.

Proof. Consider the following Lyapunov candidate

$$V_d(\boldsymbol{e}_\nu) = \frac{1}{2}\boldsymbol{e}_d^T\boldsymbol{M}\boldsymbol{e}_d. \tag{30}$$

Taking the time derivative of $V_d(\boldsymbol{e}_d)$ and using the error dynamics (28) coupled with the control law (29), we have that

$$\dot{V}_d = \boldsymbol{e}_d^T\boldsymbol{M}\dot{\boldsymbol{e}}_d = -\boldsymbol{e}_d^T\left(\boldsymbol{K}_d + \boldsymbol{D}(\boldsymbol{\nu}_r)\right)\boldsymbol{e}_d. \tag{31}$$

Knowing that $\boldsymbol{D}(\boldsymbol{\nu}_r))$ is a positive-definite matrix of damping forces, the following inequality is satisfied

$$\dot{V}_d \leq -\lambda_{\text{min}}(\boldsymbol{K}_d + \boldsymbol{D}(\boldsymbol{0}))\left\|\boldsymbol{e}_d\right\|^2, \quad \forall \boldsymbol{e}_d \in \mathbb{R}^3, \tag{32}$$

where $\boldsymbol{A} = \boldsymbol{K}_d + \boldsymbol{D}(\boldsymbol{0})$ and $\lambda_{\text{min}}(\boldsymbol{A})$ denote the smallest eigenvalue of matrix $\boldsymbol{A}$. Since $\frac{1}{2}\lambda_{\text{min}}(\boldsymbol{M})\left\|\boldsymbol{e}_d\right\|^2 \leq V_d(\boldsymbol{e}_d) \leq \frac{1}{2}\lambda_{\text{max}}(\boldsymbol{M})\left\|\boldsymbol{e}_d\right\|^2, \forall \boldsymbol{e}_d \in \mathbb{R}^3$, we have that $\boldsymbol{e}_d = \boldsymbol{0}$ is GES. □

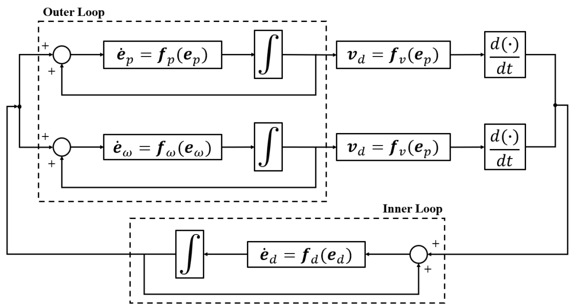

Fig. 5. Inner-outer interconnection, where the outer loop consists in two independent systems related with position and attitude.

D. Ocean Current Observer

An AUV moving through water is generally subject to ocean currents, which influence the motion of the vehicle. The intensity of such currents affects the kinematic control of the vehicle, modifying the total velocity of the vehicle itself. Such disturbances are not easy to sense, but in [8] the authors proposed a solution using the vehicle relative velocity. However, such measurements are difficult to obtain, with the common underwater velocity measurement device, i.e., Doppler Velocity Logger, being prone to errors in the mode of operation that measures such data. The other more reliable mode of operation measures true velocity readings, relative to the ocean seafloor. Therefore, our ocean current observer follows the solution proposed by the authors in [35], assuming we have such velocity readings and know the model parameters of our vehicle.

E. Inner-Outer Loop Stability

Stability is not guaranteed for inner-outer loop systems, due to the existence of interconnection terms [36]. Towards analyzing their stability, we resort to tools rooted in the input-to-state (ISS) and input-to-output stability (IOS) notions [37], [38] and variations of these, such as almost input-to-state stable (aISS) [39] for systems evolving in spaces homeomorphic to Euclidean spaces such as SO(3), or ISS with restrictions, where certain initial conditions must be satisfied. The stability analysis considers an interconnection of both systems, as shown in Fig. 5, and we assume we access to the true states of the vehicle position $\boldsymbol{p}$, velocity $\boldsymbol{\nu}$, the target position $\boldsymbol{p}_t$, with its velocity estimate $\hat{\boldsymbol{v}}_t$ provided by the tracking filter, and the ocean current velocity estimate $\hat{\boldsymbol{V}}_{c_v}$ provided by the ocean current observer.

The following theorem is established. Due to space limitations, this proof is omitted but can be found in [40].

Theorem 1. *Consider the system described by* (9) *and* (10) *in closed-loop with the following control law*

$$\boldsymbol{\tau} = -\boldsymbol{K}_d \boldsymbol{e}_d + \boldsymbol{D}(\boldsymbol{\nu}_r)\boldsymbol{\nu}_d + \boldsymbol{C}(\boldsymbol{\nu}_r)\boldsymbol{\nu}_r, \tag{33}$$

$$\boldsymbol{\omega}_d = \boldsymbol{K}_\omega \boldsymbol{S}^{-1}(\boldsymbol{R}_e \boldsymbol{Q}\boldsymbol{Q}^T - \boldsymbol{Q}\boldsymbol{Q}^T \boldsymbol{R}_e^T), \tag{34}$$

$$\begin{aligned}\boldsymbol{v}_d = &-\lambda_p \boldsymbol{\sigma}\left(\frac{k_p}{\lambda_p}\boldsymbol{e}_p\right) - \\ &- \boldsymbol{R}_v^T\left(\hat{\boldsymbol{V}}_{c_v} - \hat{\boldsymbol{v}}_t - \boldsymbol{R}_t\left(\frac{\partial \boldsymbol{p}_d^t(\gamma)}{\partial \gamma}\dot{\gamma}_d + \boldsymbol{S}(\boldsymbol{w}_t)\boldsymbol{p}_d^t(\gamma)\right)\right),\end{aligned} \tag{35}$$

$$\dot{\gamma} = \dot{\gamma}_d - k_\gamma \left(\rho_{\tilde{\gamma}}\sigma(k_{\tilde{\gamma}}\tilde{\gamma}) - \boldsymbol{e}_p^T \boldsymbol{R}_v^T \boldsymbol{R}_t^n \frac{\partial p_d^t(\gamma)}{\partial \gamma}\right), \tag{36}$$

where $\boldsymbol{K}_d$ and $\boldsymbol{K}_{p_\omega}$ are positive definite gain matrices, and k_p, $\rho_{\tilde{\gamma}}$, $k_{\tilde{\gamma}}$ and λ_p are positive parameter gains. Let $\frac{\partial \boldsymbol{p}_d^t(\gamma)}{\partial \gamma}$, $\frac{\partial^2 \boldsymbol{p}_d^t(\gamma)}{\partial \gamma^2}$ and $\boldsymbol{V}_{c_v}$ be bounded signals. Then, there are sufficiently large gains $\boldsymbol{K}_d$ such that the closed-loop system is finite-gain $\mathcal{L}$ stable, with restriction on $\boldsymbol{e}_v(0)$ and $\tilde{\boldsymbol{v}}_t(0)$ initial conditions.

VI. Results and Discussion

This section presents a simulation example to illustrate the performance of the control schemes proposed for vehicle position and attitude in the presence of parametric uncertainty and constant ocean current disturbances. The scenario consisted in having an AUV follow a moving diver, maintaining a safe distance of approximately 4 meters. The desired angular location γ_d is made to parameterize the closest point $\boldsymbol{p}_d(\gamma_d)$ between the circular path centered on the diver position, and the mission site position $\boldsymbol{p}_m$. Here we parameterize a circle, but the control system can work with other types of curve parameterizations, e.g., ellipses, taking the mission objectives in mind, extending the original work [9]. The AUV must stabilize its roll and pitch while maintaining the desired heading angle ψ_d provided by an implemented guidance system (refer to [40] for details), done in a two-fold approach: 1) while approaching the diver, the AUV must align its heading with the body surge axis; 2) near the diver, the AUV must change its heading to point towards the mission site. The AUV starts from the initial condition $\boldsymbol{\eta} = [15, 15, 30, 0, 0, 0]^T$ and $\boldsymbol{\nu} = [0, 0, 0, 0, 0, 0]^T$, and the diver initial position $\boldsymbol{p}_t = [5, 5, 20]^T$ and velocity $\boldsymbol{v}_t = [0.1, 0.1, 0]^T$. Finally, we consider that the diver position measurements are imbued with zero-mean Gaussian noise with a standard deviation of $\sigma_t = 0.4$ m in all three directions, with an observation time of 1 second, the vehicle possesses model parameter uncertainties of 10% and there exists some sort of irrotational ocean current with unknown initial values. The tracking filter is designed with a process noise variance $\sigma_q = 0.1$ and a measurement noise variance of $\sigma_x = \sigma_y = \sigma_z = 0.1$ m, following the choices of the tracking filter implement by the authors in a real ocean mission [10]. The filter target state is initialized at zero except for its position which is initialized around the initial measured target position $\boldsymbol{p}_t$. The overall scenario can be visualized in Fig. 6.

The obtained results, presented in Fig. 7, show that even under model parameter uncertainty and noisy data from the diver's position, the positioning controller can track the diver, maintaining a safe distance of around 4 meters with a maximum error of ≈0.5 meters. The tracking filter provides estimates of the diver state that ultimately allows us to not only obtain a continuously filtered version of the diver position $\hat{\boldsymbol{p}}_t$, but also the target inertial velocity estimate $\hat{\boldsymbol{v}}_t$. The oscillations

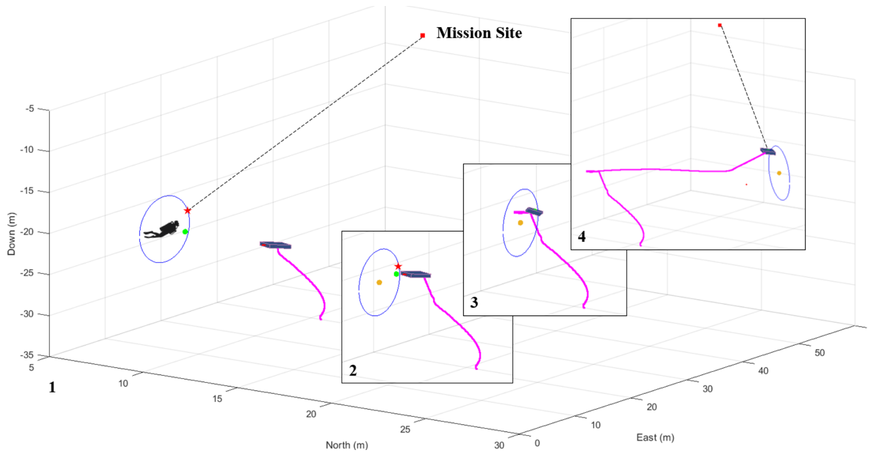

Fig. 6. In the initial approach (1), the AUV converges to the closest point $\boldsymbol{p}_d(\gamma)$, in green, between it and the diver position, in yellow, while the attitude controller keeps the roll and pitch stabilized and the heading aligned with the velocity vector. In (2), the AUV follows $\boldsymbol{p}_d(\gamma)$ along the circular path, where $\boldsymbol{p}_d(\gamma)$ is converging to the closest point between the diver and the mission site $\boldsymbol{p}_d(\gamma_d)$, as a red star. Simultaneously (3), the AUV heading changes to face the mission site. Finally (4), when the vehicle has approached the diver, it maintains its heading and follows the diver, maintaining a safe distance.

that are evidenced in the range plot, in the upper-left graph, are due to these model parameter uncertainty and noisy data, which translates into oscillations on the desired position for the AUV to follow, as expected. The attitude controller is also able to reduce the relative bearing between the AUV attitude and mission site. Moreover, due to the model uncertainty, our ocean current estimation error norm $\|\boldsymbol{e}_2\|$ is bounded and converges to a neighbourhood of the origin.

VII. Conclusions

This thesis addressed several modelling, navigation and control problems to promote cooperation synergies between a diver and an AUV. We highlighted the importance of establishing crucial mechanisms for AUV to observe and locate the diver. We presented classical and novel solutions to solve this problem of diver localization and discussed their different implementations and propose a cooperation architecture, highlighting the different systems that promote a specific cooperation strategy, and the requirements for the design of a control system. This controller was derived based on Lyapunov techniques on non-linear systems, translated into an inner-outer loop design problem of providing the desired velocities for the vehicle to achieve, to stabilize its kinematic components of attitude and position independently. Regarding the position control, a moving path-following controller was proposed to solve the problem of stabilizing the vehicle position along a desired time-independent path, with the equilibrium points satisfying GAS. The attitude control towards stabilizing at an arbitrary desired attitude was formulated as a *set-point regulation* problem, where the control design regarded the attitude error dynamics as a system evolving on $SO(3)$, with equilibria satisfying AGAS. The inner-outer loop interconnection was also analyzed and given arbitrary initial conditions, the system is always stable for a certain appropriate choice of gains. Simulation results were presented in the presence of realistic measurement noise of the diver position, unknown ocean currents and parametric uncertainty, illustrating the performance and robustness achieved with the proposed controller under the presented cooperation architecture. Future work will extend the derived controller to be more robust against parametric uncertainty in an adaptive approach such as [8] or take into account under-actuated vehicles [41], [42], develop different controller solutions to the various cooperation strategies highlighted in this work, expand the diver tracking filter taking into account velocity measurements in addition (PVM filters), a more thorough stability analysis for systems evolving in rotation manifolds by considering tangent spaces in these groups [43].

References

[1] Serena Lucrezi, Salih Egi, Massimo Pieri, Francois Burman, Tamer Ozyigit, Cialoni Danilo, G. Thomas, Alessandro Marroni, and Melville Saayman. Safety priorities and underestimations in recreational scuba diving operations: A european study supporting the implementation of new risk management programmes. *Frontiers in Psychology*, 9:383, 03 2018.

[2] Enrica Zereik, Marco Bibuli, Nikola Mišković, Pere Ridao, and António Pascoal. Challenges and future trends in marine robotics. *Annual Reviews in Control*, 46:350–368, 2018.

[3] Junhai Luo, Ying Han, and Liying Fan. Underwater acoustic target tracking: A review. volume 18, 2018.

[4] Manav Kumar and Sharifuddin Mondal. Recent developments on target tracking problems: A review. *Ocean Engineering*, 236:109558, 2021.

[5] Marco Morgado. *Advanced Ultra-Short Baseline Inertial Navigation Systems*. PhD thesis, Instituto Superior Técnico, 2011.

[6] Pedro Batista, Carlos Silvestre, and Paulo Oliveira. Single range aided navigation and source localization: Observability and filter design. *Syst. Control. Lett.*, 60:665–673, 2011.

[7] Maurice Fallon, Michael Kaess, Hordur Johannsson, and John Leonard. Efficient auv navigation fusing acoustic ranging and side-scan sonar. pages 2398–2405, 06 2011.

[8] A. Aguiar and A. Pascoal. Dynamic positioning and way-point tracking of underactuated auvs in the presence of ocean currents. *International Journal of Control*, 80(7):1092–1108, 2007.

[9] Đula n., Filip Mandić, and Nikola Misković. Diver tracking using path stabilization - the virtual diver experimental results. *IFAC-PapersOnLine*, 49(23):214–219, 2016. 10th IFAC Conference on Control Applications in Marine SystemsCAMS 2016.

[10] Matheus F. Reis, R. Praveen Jain, Pedro Aguiar, and João Borges de Sousa. Robust moving path following control for robotic vehicles: Theory and experiments. *IEEE Robotics and Automation Letters*, 4(4):3192–3199, 2019.

[11] David Cabecinhas, Rita Cunha, and Carlos Silvestre. Almost global stabilization of fully-actuated rigid bodies. *Systems and Control Letters*, 58(9):639–645, 2009.

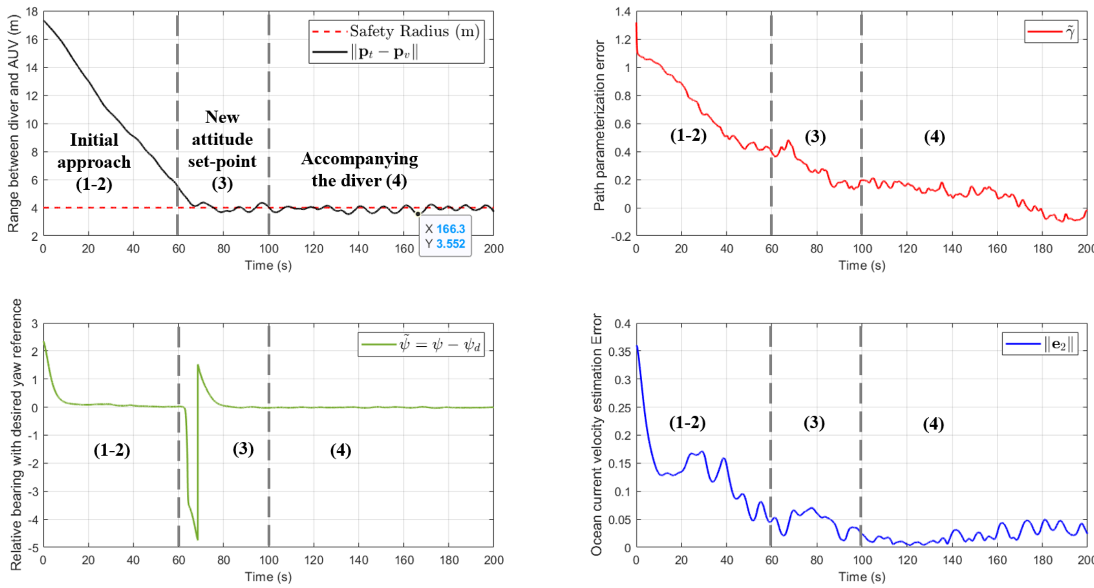

Fig. 7. Evolution in time of the different estimation error variables and position/attitude errors.

[12] P. Maurya, A. Pedro Aguiar, and A. Pascoal. Marine vehicle path following using inner-outer loop control. *IFAC Proceedings Volumes*, 42(18):38–43, 2009. 8th IFAC Conference on Manoeuvring and Control of Marine Craft.

[13] Deliverable D 1.1 Requirements Analysis Report. Cooperative cognitive control for autonomous underwater vehicles. http://robotics.jacobs-university.de/projects/Co3-AUVs/publicdeliverables/D11-RequirementsAnalysis.pdf.

[14] Project swarms - smart and networking underwater robots in cooperation meshes. http://www.swarms.eu/. Accessed: 2021-09-09.

[15] Cognitive robotics: Cooperative control and navigation of multiple marine robots for assisted human diving operations. https://cordis.europa.eu/project/id/255216. Accessed: 2021-09-20.

[16] Geert De Cubber and Daniela Doroftei. *Search and Rescue Robotics - From Theory to Practice*. 08 2017.

[17] Nikola Miskovic, Marco Bibuli, Andreas Birk, Massimo Caccia, Salih Egi, Karl Grammer, Alessandro Marroni, Jeffrey Neasham, Antonio Pascoal, Antonio Vasilijevic, and Zoran Vukić. Caddy—cognitive autonomous diving buddy: Two years of underwater human-robot interaction. *Marine Technology Society Journal*, 50:54–66, 07 2016.

[18] Alfonso Gómez-Espinosa, Enrique Cuan-Urquizo, and Josué González-García. Autonomous underwater vehicles: Localization, navigation, and communication for collaborative missions. *Applied Sciences*, 10:1256, 02 2020.

[19] Enrico Simetti, Stefano Galeano, and Giuseppe Casalino. Underwater vehicle manipulator systems: Control methodologies for inspection and maintenance tasks. pages 1–7, 04 2016.

[20] Stephanie Wehkamp and Philipp Fischer. Impact of coastal defence structures (tetrapods) on a demersal hard-bottom fish community in the southern north sea. *Marine environmental research*, 83, 11 2012.

[21] Chris Chesher. Robots and the moving camera in cinema, television and digital media. volume 9549, pages 98–106, 07 2016.

[22] Dariusz Jóźwiak, Piotr Siermontowski, Zbigniew DąbrowieckiI, and Romuald Olszański. Analysis of the risk of diving accidents in military and recreational diving. *Polish Hyperbaric Research*, 53(4), 2016.

[23] Kenshi Saho. Kalman filter for moving object tracking: Performance analysis and filter design. 02 2018.

[24] Bertil Ekstrand. Some aspects on filter design for target tracking. *Journal of Control Science and Engineering*, 2012, 05 2012.

[25] W. Nodland, T. Ewart, W. Bendiner, J. Miller, and E. Aagaard. Spurv ii-an unmanned, free-swimming submersible developed for oceanographic research. In *OCEANS 81*, pages 92–98, 1981.

[26] Hwee-Pink Tan, Roee Diamant, Winston K.G. Seah, and Marc Waldmeyer. A survey of techniques and challenges in underwater localization. *Ocean Engineering*, 38(14):1663–1676, 2011.

[27] P H Milne. *Underwater acoustic positioning systems*. Gulf Publishing Company, 1 1983.

[28] André B. Figueiredo, Bruno M. Ferreira, and Aníbal C. Matos. Tracking of an underwater visual target with an autonomous surface vehicle. In *2014 Oceans - St. John's*, pages 1–5, 2014.

[29] Tiedong Zhang, Shuwei Liu, Xiao He, Hai Huang, and Kangda Hao. Underwater target tracking using forward-looking sonar for autonomous underwater vehicles. *Sensors*, 20(1), 2020.

[30] Nguyen T. Hung, Francisco F. C. Rego, and António Pascoal. Cooperative distributed estimation and control of multiple autonomous vehicles for range-based underwater target localization and pursuit. *IEEE Transactions on Control Systems Technology*, pages 1–15, 2021.

[31] T. I. Fossen. *Handbook of Marine Craft Hydrodynamics and Motion Control*. Wiley, first edition, 05 2011.

[32] Alberto Isidori, Lorenzo Marconi, and Andrea Serrani. *Robust Autonomous Guidance: An Internal Model Approach*. Springer, October 2003.

[33] Rita Cunha. *Advanced Motion Control for Autonomous Air Vehicles*. PhD thesis, Instituto Superior Técnico, 2007.

[34] Daniel Koditschek. The application of total energy as a lyapunov function for mechanical control systems. *Contemporary Mathematics, American Mathematical Society, 1989*, 97, 02 1989.

[35] Even Børhaug, Luca Pivano, Kristin Y. Pettersen, and Tor Arne Johansen. A model-based ocean current observer for a 6dof underwater vehicle. *IFAC Proceedings Volumes*, 40(17):169–174, 2007. 7th IFAC Conference on Control Applications in Marine Systems.

[36] Isabelle Fantoni, Rogelio Lozano, and Farid Kendoul. Asymptotic stability of hierarchical inner-outer loop-based flight controllers. *IFAC Proceedings Volumes*, 41(2):1741–1746, 2008. 17th IFAC World Congress.

[37] Eduardo D. Sontag and Yuan Wang. A notion of input to output stability. pages 3862–3867, 1997.

[38] Hassan K Khalil. *Nonlinear systems*. Prentice-Hall, Upper Saddle River, NJ, third edition, 2002.

[39] David Angeli and Laurent Praly. Stability robustness in the presence of exponentially unstable isolated equilibria. *IEEE Transactions on Automatic Control*, 56(7):1582–1592, 2011.

[40] André Potes. Cooperation of humans and robots underwater. Master's thesis, 2021. Instituto Superior Técnico, Lisbon, Portugal.

[41] Pedro Aguiar, João Almeida, Behzad Bayat, Bruno Cardeira, Rita Cunha, Andreas Häusler, Pramod Maurya, A. Oliveira, Antonio Pascoal, Arvind Pereira, Manuel Rufino, Luis Sebastiao, Carlos Silvestre, and F. Vanni. Cooperative autonomous marine vehicle motion control in the scope of the eu grex project: Theory and practice. pages 1 – 10, 06 2009.

[42] Francesco Vanni. *Coordinated Motion Control of Multiple Autonomous Underwater Vehicles*. PhD thesis, Instituto Superior Técnico, 2007.

[43] Jari Mäkinen. Rotation manifold so(3) and its tangential vectors. *Computational Mechanics*, 42:907–919, 11 2008.